time axis. Convolution with the IRF also has the added benefit of smoothing out the statistical variations of the Monte-Carlo model. A gain factor G is introduced to account for the measured arbitrary amplitude output by the system. Fitting of $\mathbf{m}$ to the measurement vector $\mathbf{y}_c$ was achieved by varying the three floating parameters (μ_a, μ_s', G) to optimize the goodness-of-fit, criteria $\chi^2 = \sum_n (y_{cn} - m_n)^2$, using the Levenberg-Marquardt algorithm. A very stringent fit window, defined as 1% of signal peak for both the rising edge and the falling edge of the trace, was selected. Figure 4. shows typical fit results obtained with our characterization procedure. The RMS value of the residuals (shown magnified by a factor of 10) is less than 0.3% of the maximum amplitude of the signal.

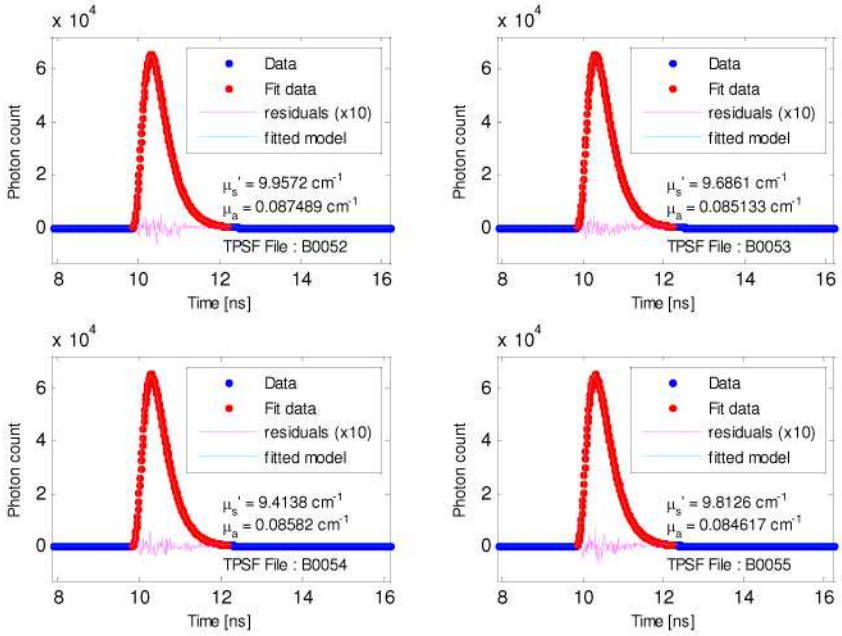

Fig. 4. Fit results for cylindrical samples coming from 4 separate batches B0052, B0053, B0054 and B0055 of our phantom production samples collection [19]. Note that the residuals have been magnified by a factor of 10.

3. Error analysis: Sources of random errors

3.1 Measurement noise

Short term random fluctuations in a measured TCSPC trace come from the shot noise associated with the optical signal itself and the dark counts. Measurement noise can be modeled but an experimental determination is more straightforward and convincing. The effect of measurement noise was therefore estimated by measuring 4 TPSF traces in sequence for six different samples. The averaged standard deviation of the fitted optical properties for each sample was $\Delta\mu_a = 0.0006\ \text{cm}^{-1}\ (0.7\%)$ and $\Delta\mu_s' = 0.027\ \text{cm}^{-1}\ (0.3\%)$.

3.2 System repeatability

A general system repeatability experiment was conducted to quantify variation that can occur when the complete measurement sequence is repeated from powering up to final sample TPSF measurement. The following sequence has been repeated five times for a single sample:

a) power up the system and wait five minutes for warm-up,

b) measure the IRF,

#125247 - $15.00 USD Received 10 Mar 2010; revised 22 Apr 2010; accepted 6 May 2010; published 14 May 2010

c) insert the sample in the sample holder,

d) measure the sample TPSF,

e) repeat step c) and d) three times randomly rotating the sample each time,

f) shut down the system.

The standard deviation obtained from all 15 measurements (five repetitions times three random orientations) is $\Delta\mu_a = 0.0017\,\mathrm{cm}^{-1}\,(1.8\%)$ for the absorption coefficient and $\Delta\mu_s' = 0.12\,\mathrm{cm}^{-1}\,(1.2\%)$ for the reduced scattering coefficient.

3.3Instrument response function (IRF) instability

The system response can drift between the IRF measurement and the sample measurement. To minimize the error introduced by this instability, a measurement of the IRF is performed at the beginning of the phantom characterization session. An upper bound to the contribution of the IRF instability to the total uncertainty has been determined by analyzing a single TPSF trace with 20 instrument response functions acquired over a time period of 4 hrs (see Fig. 5). The IRF instability contribution to the total error has been determined by taking the standard deviation of the 20 retrieved optical properties. This procedure was repeated for TPSF traces measured on 4 different phantoms samples. The average of the standards deviations obtained from the 4 repetition gives an IRF instability contribution of $\Delta\mu_a = 0.0005\,\mathrm{cm}^{-1}\,(0.62\%)$ for the absorption coefficient and $\Delta\mu_s' = 0.04\,\mathrm{cm}^{-1}\,(0.4\%)$ for the reduced scattering coefficient. These error estimates are conservative since multiple samples can be measured within a 10 minutes time frame.

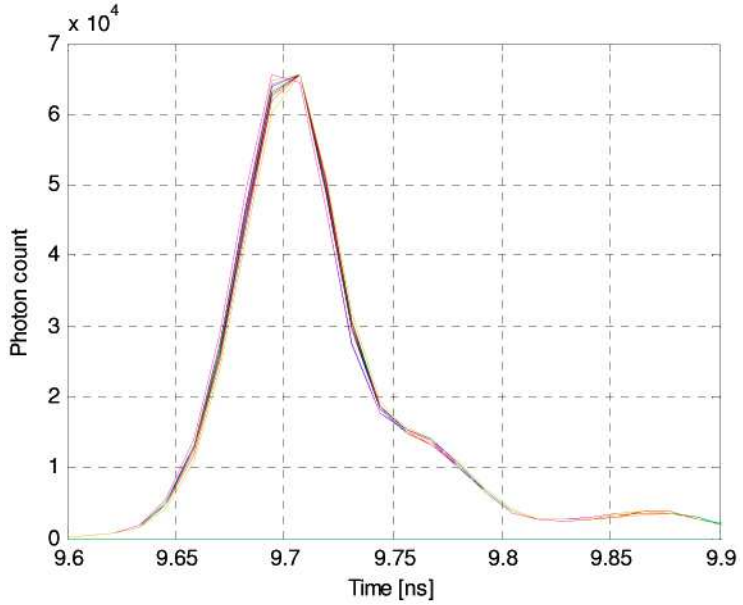

Fig. 5. Instrument response functions acquired over a 4 hr time period

4. Error analysis: Sources of systematic errors

4.1 Sample thickness inaccuracy

Our batch characterization samples are machined to a cylindrical shape with a certain degree of dimensional accuracy. By taking the standard deviation of the measured thickness of 80 standard samples (see section 2.1), we have determined the accuracy in thickness to

#125247 - $15.00 USD Received 10 Mar 2010; revised 22 Apr 2010; accepted 6 May 2010; published 14 May 2010

be $\Delta d = 300\mu m$. Our data analysis is based on pre-computed TPSF traces from a Monte-Carlo model that assumes a nominal sample thickness of 20 mm. The sample thickness variation, even though it can be characterized to a high level of accuracy, is not taken into account in our analysis and induces a bias on the optical properties. The magnitude of this bias was estimated by fitting an experimental trace using both a correct (case 1) and an erroneous (case 2) sample thickness, d_0 and $d_0 + 300\mu m$ respectively, and determining the difference in the obtained optical properties. A diffusion approximation, DA, slab model [7] was used to allow free variation of the sample thickness. The error estimate therefore assumes that the bias induced by the use of the DA is common to both cases and thus subtracts out when taking the difference in retrieved optical properties. The process was repeated with the 4 experimental traces shown in Fig. 4. The average of the bias values obtained for the 4 traces gives sample thickness inaccuracy bias estimates of $\Delta\mu_a = 0.001\,\mathrm{cm}^{-1}\,(1.1\%)$ and $\Delta\mu_s' = 0.25\,\mathrm{cm}^{-1}\,(2.5\%)$.

4.2 Refractive index inaccuracy

Error in the evaluation of the refractive index of the bulk sample has a direct impact on the recovered optical properties. As described in [19], the refractive index of the polyurethane used for phantoms fabrication was determined by a time-of-flight experiment. The value obtained for the refractive index was $n = 1.521 \pm 0.006$.

The impact of this refractive index uncertainty on the retrieved optical properties uncertainty was evaluated in a similar fashion for the sample thickness inaccuracy. 4 experimental traces were analyzed with both the correct and the erroneous values of the refractive index. Retrieved optical properties for each index value were then subtracted to obtain the biases induced by the refractive index inaccuracy. The average of the bias values obtained for the 4 traces gives a refractive index inaccuracy bias estimate of $\Delta\mu_a = 0.001\,\mathrm{cm}^{-1}\,(1.1\%)$ and $\Delta\mu_s' = 0.035\,\mathrm{cm}^{-1}\,(0.35\%)$.

4.3 Anisotropy factor inaccuracy

Error in the evaluation of the anisotropy factor *g* may also impact the recovered optical properties. The *g* factor used in the Monte-Carlo model was determined experimentally as described in [19]. In brief, phantom batches with TiO_2 particles but no absorber were prepared and machined into thin wedges in addition to our standard characterization cylinders. The thickness of the wedged samples was selected to insure single scattering regime in transmission. The anisotropy factor was calculated using $g = 1 - \mu_s'/\mu_s \approx 1 - \mu_s'/\mu_t$ which neglects the small contribution of absorption to the total attenuation μ_t because no absorber was used. The total attenuation coefficient of a given batch was determined by measuring the coherent (non-scattered) transmission of the thin wedges. Samples were wedged to allow measurements at differential thicknesses on the same sample to experimentally factor out the contribution of Fresnel reflection at the interfaces. μ_s' was determined by characterizing the standard cylinders coming from the same batch using the technique described in section 2 assuming a *g* value of 0.59. The mean value of the anisotropy factor obtained for the various TiO_2 concentration was $g = 0.62 \pm 0.015$. The uncertainty on *g* was calculated using the μ_s' inaccuracy value obtained in this paper (see section 5) and the μ_t standard deviation observed experimentally.

To evaluate the possible impact of this uncertainty on the retrieved optical properties, Monte-Carlo simulations were used to generate traces for *g* values excursion of 0.015. These traces were then treated like experimental input vectors to recover the optical properties using our reference database (which assumes a *g* value of 0.62). The dependence on the *g* value was

#125247 - $15.00 USD Received 10 Mar 2010; revised 22 Apr 2010; accepted 6 May 2010; published 14 May 2010

found to be relatively weak. The average of the bias values are of $\Delta\mu_a = 0.0001\,\mathrm{cm}^{-1}\,(0.1\%)$ and $\Delta\mu_s' = 0.003\,\mathrm{cm}^{-1}\,(0.03\%)$.

4.3 Time base inaccuracy

The time axis of a TCSPC trace is determined by the system's time-to-analog (TAC) converter. This electronics component (internal to the TCSPC system) measures the time between a photon detection event and a reference synchronization pulse by integrating a current source in a capacitor, therefore converting a time delay into a voltage that can be digitized into a numerical value. TCSPC system time bases are calibrated by the manufacturer by sending pulses with known delays to the CFD (detector) input and the synchronizing input using a delay generator. The calibration error in this time base is estimated to be 1% according to the manufacturer [25]. The implication of this unknown time stretching on the uncertainty in the retrieved optical properties has been estimated by using a stretched version of the time axis vector, $t' = 1.01 \cdot t$, for computing the theoretical TPSF from the Monte-Carlo model. The stretching of the axis resulted in offsets of $\Delta\mu_s' = 0.07\,\mathrm{cm}^{-1}\,(0.7\%)$ and $\Delta\mu_a = 0.0015\,\mathrm{cm}^{-1}\,(1.7\%)$ in the optical properties.

4.4 Forward model inaccuracy

The chosen approach to evaluate the limitations of the model is to compare the recovered optical properties from phantoms of various shapes and sizes made from a single batch of polyurethane mix. Two complete phantom sets of equal reduced scattering coefficients (~10 cm^{-1}) but different absorption coefficients (approximately 0.07 cm^{-1} and 0.16 cm^{-1}) were casted into molds and machined into cylinder and rectangular blocks for a total of six different geometries (Fig. 6.). More details about our phantom fabrication process including scatterer and absorber calibrations can be found in [19,17]. This phantom set allows evaluation of the model dependence with respect to two geometrical parameters: lateral size and thickness.

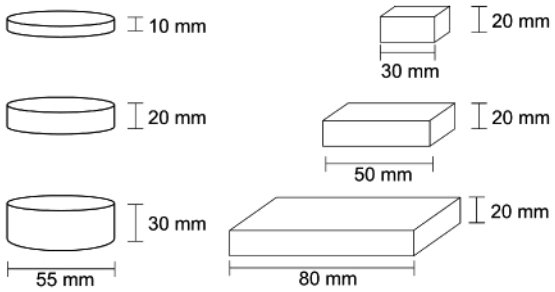

Fig. 6. Phantom set fabricated from a single batch to evaluate the model limitations

Each phantom was characterized using a Monte-Carlo model taking into account its specific geometry, as described in section 2.3. Proper modeling of the light escaping from the sides of the phantom gets particularly important as the lateral size is reduced. For example, results from our simulations are showing that given $\mu_s' = 10\,\mathrm{cm}^{-1}$, approximately 20% of the incoming light is lost in this manner for the 30 mm wide rectangular phantom. For each sample, three TPSF were acquired with the light beam normally incident on its center. Averages of the recovered optical properties are compiled in Table 1.

#125247 - $15.00 USD Received 10 Mar 2010; revised 22 Apr 2010; accepted 6 May 2010; published 14 May 2010

Table 1. Characterization results for all phantoms

Geometry	Size	Thickness	Low absorption batch		High absorption batch	
			μ_a	μ_s'	μ_a	μ_s'
	mm	mm	cm^{-1}	cm^{-1}	cm^{-1}	cm^{-1}
Cyl	55	10	0.060	9.08	0.146	8.82
Cyl	55	20	0.069	9.28	0.161	9.15
Cyl	55	30	0.071	9.49	0.164	9.32
Rec	30	20	0.072	9.50	0.162	9.33
Rec	50	20	0.070	9.45	0.162	9.35
Rec	80	20	0.070	9.46	0.160	9.20
		Mean	**0.069**	**9.38**	**0.159**	**9.20**
		Std. dev.	**0.0042**	**0.17**	**0.0064**	**0.20**
		% variation	**6.2%**	**1.8%**	**4.0%**	**2.2%**

As evidenced in Fig. 7. (left graphs), minimal dependence on the lateral dimension of the rectangular samples is observed. This suggests that boundary conditions are properly modeled in the modified MCML code. However, the model appears not as robust with respect to phantom thickness. When plotted against sample thickness, the recovered absorption and scattering coefficients (Fig. 7., right graphs) show a clear trend that cannot be attributed to measurement noise. The highest relative variability, expressed as the standard deviation of the values over the mean, is observed for the μ_a results of the low absorption set.

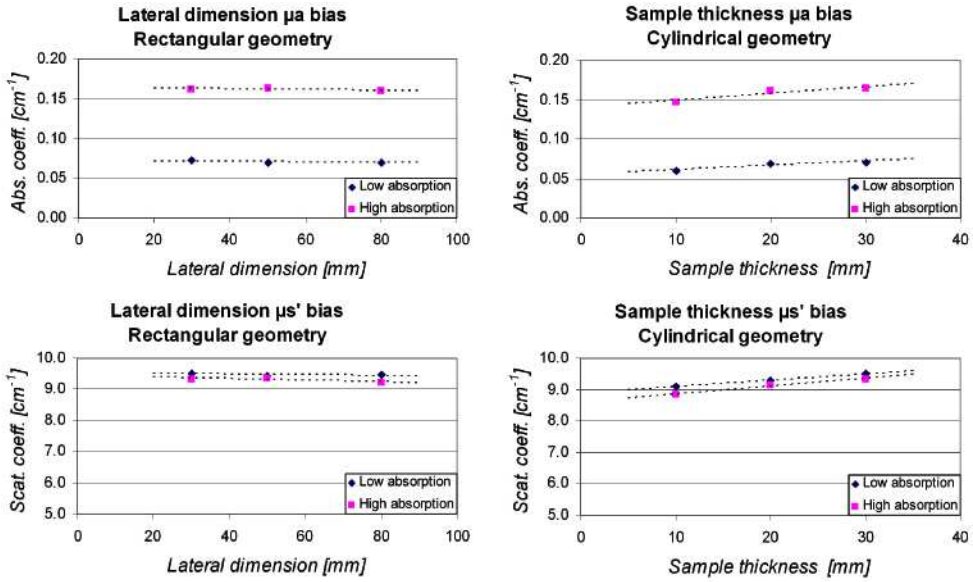

Fig. 7. μ_a and μ_s' dependence on the sample's lateral dimension and thickness

5. Error analysis budget

Summarized in Table 2 are the estimated results of the random and systematic error sources evaluated in this work. Worst case values were selected for each contribution. A 2 sigma root mean square sum of all contributor gives uncertainties of $\Delta\mu_a\big|_{2\sigma} = 0.01\,\text{cm}^{-1}\,(11.3\%)$ and $\Delta\mu_s'\big|_{2\sigma} = 0.67\text{cm}^{-1}\,(6.8\%)$. It is to be noted that the precision of the technique (its ability to detect small relative changes in the optical properties), is only affected by the random fluctuations for which an RSS sum gives $\Delta\mu_a\big|_{2\sigma\,\text{md only}} = 0.0017\,\text{cm}^{-1}\,(2\%)$ and

#125247 - $15.00 USD Received 10 Mar 2010; revised 22 Apr 2010; accepted 6 May 2010; published 14 May 2010

$\Delta\mu_s'|_{2\sigma\,\mathrm{rnd\,only}} = 0.13\mathrm{cm}^{-1}(1.3\%)$. The technique is therefore very sensitive to small changes in the optical properties. Highly accurate values of the ratio of optical properties could therefore be obtained since the systematic portion of the errors would cancel out. Ratios of absorption or reduces scattering coefficient could be calculated between two phantoms or between to values obtained at different wavelengths for the same phantom.

Table 2. Contribution of errors

Error source	Absolute error (cm^{-1})		Relative error (%)*	
	μ_a	μ_s'	μ_a	μ_s'
Random error sources				
Measurement noise	0.0006	0.027	0.71%	0.27%
System repeatability	0.0017	0.12	1.8%	1.2%
IRF instabilities	0.0005	0.04	0.59%	0.4%
Systematic error sources				
Sample thickness	0.001	0.25	1.18%	2.5%
Refractive index	0.001	0.035	1.18%	0.35%
Anisotropy factor	0.0001	0.003	0.1%	0.03%
Time base inaccuracies	0.0015	0.07	1.76%	0.7%
Monte-Carlo model	0.004**	0.20	4.71%	2.2%
Total error (RSS, 1σ)	**0.005**	**0.34**	**5.7%**	**3.4%**
Total error (RSS, 2σ)	**0.010**	**0.67**	**11.3%**	**6.8%**

* relative to μ_a = 0.085 cm^{-1} and μ'_s = 10 cm^{-1}

** The standard deviation of μ_a obtained from the low absorption series of the sample geometry experiment (see Table 1) was selected because the mean absorption coefficient (0.069 cm^{-1}) was closer to the mean absorption coefficient of the other samples that were used for estimating the other error contributions (0.085 cm^{-1}).

6. Conclusion

The primary objective here was to evaluate the absolute accuracy of determined optical properties from a solid phantom when using the time resolved transmittance measurement method. The random contribution of measurement noise and IRF instability could be reduced by averaging multiple measurements. The sample thickness contribution could be reduced by tighter manufacturing tolerances on the dimensions of the test sample. Generation of a 2-parameter TPSF database that can be interpolated for a measured thickness and scattering coefficient is also an effective strategy for reducing this contribution. Refinement to the refractive index measurements and time base accuracy evaluations can also be explored, but the largest error contributor remains the model inaccuracy. However, improvement on the robustness of the model can be non trivial. Bias imposed by boundary effects, the sample thickness correction, and the RTE modeling have already been taken into account. Investigation of the root cause of the remaining biases will be the focus of future efforts. Once those last issues are resolved, the proposed technique and data analysis presented herein could serve as a standard method to determine the optical properties of turbid tissue-mimicking media.

#125247 - $15.00 USD Received 10 Mar 2010; revised 22 Apr 2010; accepted 6 May 2010; published 14 May 2010